

Dissociative Intramolecular Charge Transfer after Local Two-Photon Ionization of Ferrocene Derivatives with Aromatic Chromophores

J. E. Braun and H. J. Neusser*

Institut für Physikalische und Theoretische Chemie, Technische Universität München, Lichtenbergstrasse 4, D-85748 Garching, Germany

P. Härter and M. Stöckl

Institut für Anorganische Chemie, Technische Universität München, Lichtenbergstrasse 4, D-85748 Garching, Germany

Received: August 20, 1999; In Final Form: December 15, 1999

Experimental evidence for dissociative intramolecular charge transfer processes is found for gas-phase ferrocene-aniline derivatives after local ionization at the aniline chromophore site via intermediate states with predominant aniline character. The direct ionization at the ferrocene site can be excluded since there is a rapid dissociation of ferrocene in the intermediate state prior to ionization so that no ferrocene ions would be produced in this case. Because of the higher local ionization energy of the chromophore, charge transfer takes place after local ionization. The released energy and additional photon absorption leads to breaking of bonds and results in a dissociation into intact ferrocene or ferrocene-containing cations and neutral fragments.

1. Introduction

Organometallic compounds, especially ferrocene and its derivatives, have attracted great interest as they represent a link between inorganic and organic chemistry and offer numerous applications.¹ Ferrocene, [bis(cyclopentadienyl)]iron(II); Fe-(C₅H₅)₂ or Fe(cp)₂ (see Figure 1, 1a), was discovered in 1951,² it is an organometallic sandwich compound, whose photophysical properties have been investigated by various groups (see ref 1 and references therein). Due to its remarkable chemical stability and the well-established methods for its incorporation into more complex structures, ferrocene has become a versatile building block for the synthesis of novel substances with unusual physical properties. Ferrocene-containing substances have been used for the investigation of charge-transfer processes in the solid and liquid phase.³ In this work, photoinduced charge-transfer experiments in a supersonic molecular beam, carried out with special tailor-made ferrocene derivatives, are described.

In a series of multiphoton dissociation (MPD)/multiphoton ionization (MPI) studies of ferrocene^{4–12} with nanosecond (ns) laser pulses at different wavelengths in the visible and near UV (UV/VIS) it has been shown that the cyclopentadienyl (cp) ligands are lost prior to ionization, and as a consequence, no intact ferrocene cations can be observed in the mass spectra. In the intensive laser radiation field the central iron atom loses its cp rings in one or more MP steps, and the uncaged iron atom can be ionized and detected by a MPI process when the laser wavelength is close to an atomic resonance. The detailed mechanism of photon absorption, energy redistribution, and dissociation has not been unequivocally established. It was concluded that the dynamics of the dissociation process depends on the chosen photon energy as well as the laser fluence. Kimura and co-workers⁸ found that the conversion of electronic to vibrational energy occurs on a faster time scale than a cp elimination. On the other hand, in two earlier publications a fast dissociation mechanism via electronic repulsive states was

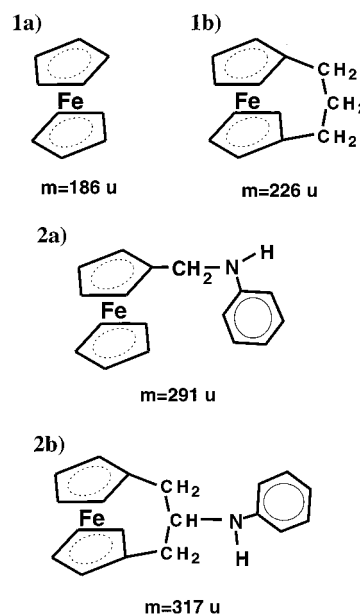


Figure 1. Ferrocene derivatives investigated in this work: 1a) Ferrocene. 1b) [3]Ferrocenophane. 2a) *n*-(Ferrocenylmethyl)aniline. 2b) 2-(*n*-Phenyl)amino-[3]-Ferrocenophane.

proposed by Liou et al.^{9,10} So, two competing dissociation mechanisms, one via statistical redistribution, the other via direct dissociation, are thought to be possible.

From thermochemical studies^{5,13,14} the dissociation energy E_2 , for the decomposition of ferrocene into a neutral iron atom and two cp radicals, is 6.2 eV. Elimination of only one cp ring requires an energy of $E_1 = 4$ eV⁵ which is noticeably more than necessary for removing the remaining second cp ring.

While resonance-enhanced two-photon ionization with typical photon energies $h\nu \leq 6.2$ eV failed to produce parent ions, one-photon vacuum ultraviolet (VUV) ionization of ferrocene leads

to intact parent (ferrocene) ions. Determination of the IE of ferrocene by one-photon VUV ionization or electron impact yielded slightly different values of 6.75 eV,⁷ 6.72 eV (adiabatic) and 6.86 eV (vertical),¹⁵ and 6.99 eV.¹² In our work, the value of 6.75 eV for the adiabatic ionization energy (AIE) is adopted. This value is 0.55 eV above the dissociation energy E_2 .

We would like to point out that soft ionization of ferrocene with a two-photon process because of a fast dissociation in the intermediate state is not possible but that the detailed mechanism of dissociation is of minor importance in our experiment. Therefore, in the ferrocene derivatives containing a chromophore used in this work, we can exclude any direct local ionization at the ferrocene site. The investigated ferrocene derivatives (see Figure 1, parts 2a and 2b) basically consist of a ferrocene or [3]ferrocenophane (1,1'-(1,3-propanediyl)ferrocene) (see Figure 1, parts 1a and 1b, respectively) unit attached to a chromophore molecule with distinct spectroscopic properties. The clear distinction of different excitation pathways at the ferrocene site and the chromophore site is crucial for our investigations of charge transfer processes after local ionization of a chromophore moiety with the higher local IE.

2. Experimental Section

2.1. Ferrocene Derivatives. The ferrocene derivatives have to fulfill several conditions to be suitable for our purposes to detect charge transfer processes. The chromophore molecule has to show strong absorption in a spectral range where the absorption coefficient of ferrocene is relatively weak. Moreover the chosen ferrocene derivative should have sufficient gas pressure at moderate temperatures and decompose only negligibly when heated and vaporized. Among various synthesized derivatives we found two suitable compounds with an aniline-like chromophore. In Figure 1 the structures of different ferrocenes are shown. In Figure 1, part 1a, the ferrocene molecule is displayed, and in Figure 1, part 1b, the ferrocenophane (bridged ferrocene) is shown. The chemical structures of the derivatives with chromophore aniline are shown in Figure 1, parts 2a, and 2b respectively: (2a) *n*-(ferrocenylmethyl)aniline (2b) 2-(*n*-phenyl)amino-[3]-ferrocenophane. The main difference between the two molecules 2a and 2b in Figure 1 is that in 2a the aniline chromophore is attached to one cp ring whereas in the case of 2b the aniline is bound to the handle that connects the two cp rings. The idea behind this selection of structures was that the charge produced after local ionization of the aniline site moves along different paths between the moieties of the respective molecules and, thus, any effects caused by the different migration paths can be examined.

2.1.1. Synthesis of *n*-(ferrocenylmethyl)aniline. This compound was synthesized according to the literature¹⁶ and purified by recrystallization from *n*-hexane prior to use.

2.1.2. 2-(*n*-Phenyl)amino-[3]-Ferrocenophane ([3]-Ferrocenophan-2-Phenylamine). [3]-Ferrocenophane-2-Phenylamine (precursor). 600 mg (2.5 mmol) of [3]-ferrocenophan-2-one¹⁷ are placed in a 100 mL round-bottom flask together with ca. 50 mg anhydrous ZnCl₂ and 5 g of molecular sieves (4 Å). Subsequently, 0.45 mL (5 mmol) aniline and 40 mL dry toluene are added. The reaction mixture is refluxed for 12 h and filtered after cooling to room temperature. After extraction of the residue twice with 10 mL of toluene the combined extracts are freed of solvent. The resulting yellow powder is recrystallized from CH₂Cl₂/*n*-hexane yielding 615 mg (78%) of yellow crystals.

Mp. 174 °C; elementary analysis (mw (C₁₉H₁₇FeN): 315.20) calcd.: C 72.40, H 5.44, Fe 17.72, N 4.44%. Found: C 72.19,

H 5.40, Fe 17.54, N 4.58%. IR (KBr, cm⁻¹): ν = 1646 (s, ν (C=N)); MS (CI, %): m/z = 315 (100, M⁺); 212 (68, M⁺-CNPh); UV/VIS (CH₂Cl₂, nm): λ_{\max} (ϵ) = 442 (250); 354 (2600); 284 (27 000); 232 (38 000); ¹H NMR (C₆D₆, 400.13 MHz, ppm): δ = 7.19 (t, 2H, m-Ph, ³J_{HH} = 7.4 Hz); 6.94 (t, 1H, p-Ph, ³J_{HH} = 7.4 Hz); 6.83 (d, 2H, o-Ph, ³J_{HH} = 7.5 Hz); 4.03 (s, 4H, C₅H₄); 3.95 ("t", 2H, C₅H₄); 3.81 ("t", 2H, C₅H₄); 2.92 (s, 2H, CH₂); 2.54 (s, 2H, CH₂); ¹³C NMR (C₆D₆, 100.63 MHz, ppm): δ = 171.4 (C=N); 151.6 (i-Ph); 129.3 (m-Ph); 123.3 (p-Ph); 119.9 (o-Ph); 76.6; 76.3 (i-C₅H₄); 70.2; 70.0; 70.0; 69.9 (C₅H₄); 37.1; 27.7 (CH₂).

2-(*N*-Phenyl)amino-[3]-Ferrocenophane. To 38 mg (1 mmol) LiAlH₄ in 10 mL of dry diethyl ether a solution of 315 mg (1 mmol) [3]-ferrocenophan-2-phenylimine in 50 mL dry diethyl ether is added dropwise. After addition of the substrate the reaction is stirred for 2 h at ambient temperature. For the workup the reaction mixture is cooled in an ice bath, and very carefully ice water is added dropwise to the reaction mixture. After the H₂ evolution has ceased the organic phase is decanted and the water phase is extracted twice with diethyl ether. The combined ether extracts are washed with 20 mL of a saturated NaCl solution, separated, and dried. After evaporation of the solvent the residue is recrystallized from *n*-hexane yielding 301 mg (95%) of orange crystals.

Mp. 165–167 °C. Mw: 317.21 g/mol (C₁₉H₁₉FeN) EA (%): calcd.: C 71.94, H 6.03, Fe 17.60, N 4.42, found: C 71.98, H 6.10, Fe 17.48, N 4.63; IR (KBr, cm⁻¹): ν = 3379 (s, ν (NH), st); 3077 (m, ν (CH), st, Cp); 1599 (s, ν (C=C), st); 1503 (s, ν (C=C), st); MS (CI, %): m/z = 317 (100, M⁺); 238 (41, M⁺-MeCp); 214 (5, M⁺-CNPh); 158 (2, M⁺-CNPh-Fe); 135 (12, M⁺-CNPh-MeCp); UV/VIS (CH₂Cl₂, nm): λ_{\max} (ϵ) = 442 (240); 298 (4600); 284 (7200); 250 (29 000); 232 (38 000); ¹H NMR (CD₂Cl₂, 400.13 MHz, ppm): ϵ = 7.19 (t, 2H, m-Ph, ³J_{HH} = 7.2 Hz); 6.68 (m, 3H, o- + p-Ph); 4.11 (s, 4H, C₅H₄); 4.07 ("t", 2H, C₅H₄); 4.03 ("t", 2H, C₅H₄); 3.91 (br, 1H, NH); 3.82 (tt, 1H, CH, ³J_{HH} = 3.0/11.1 Hz); 2.71 (dd, 2H, CHH_{cis}, ²J_{HH} = 13.8 Hz, ³J_{HH} = 2.6 Hz); 1.71 (dd, CHH_{trans}, ²J_{HH} = 13.8 Hz, ³J_{HH} = 11.2 Hz). ¹³C NMR (CD₂Cl₂, 100.63 MHz, ppm): ϵ = 147.6 (i-Ph); 129.7 (m-Ph); 117.6 (p-Ph); 113.3 (o-Ph); 82.0 (i-C₅H₄); 71.6; 69.6; 68.4; 68.3 (C₅H₄); 60.6 (CH); 32.1 (CH₂).

2.1.3. Laser Mass Spectrometry. The experimental setup used was described in detail elsewhere.¹⁸ Briefly, it consists of two dye lasers yielding light pulses with a bandwidth of ~ 0.3 cm⁻¹ (fwhm) and a duration of ~ 15 ns (fwhm) (FL 3002, and LPD 3000; Lambda Physik). The dye lasers are pumped synchronously by a XeCl excimer laser (EMG 1003i, Lambda Physik). The two counter-propagating laser beams intersect a skimmed supersonic molecular beam perpendicularly 15 cm downstream from the nozzle orifice. The light pulses overlap in time and space in the acceleration region of a linear reflecting time-of-flight mass spectrometer.¹⁹ The supersonic jet is obtained by expanding argon carrier gas with a backing pressure of 3 bar into the vacuum with a heated, pulsed (10 Hz repetition rate) valve. The samples of the investigated ferrocenes were heated to 160 °C in a sample chamber close to the nozzle of the valve. At this temperature, little thermal decomposition of the investigated ferrocene derivatives takes place. After the experiment, the remaining substances were removed and analyzed by NMR and electron impact mass spectrometry. No products originating from thermal decomposition could be found. To check if sufficient amounts of the substances were evaporated, mass spectra with sharply focused laser light at the highest available laser power were recorded, thus forcing complete fragmentation

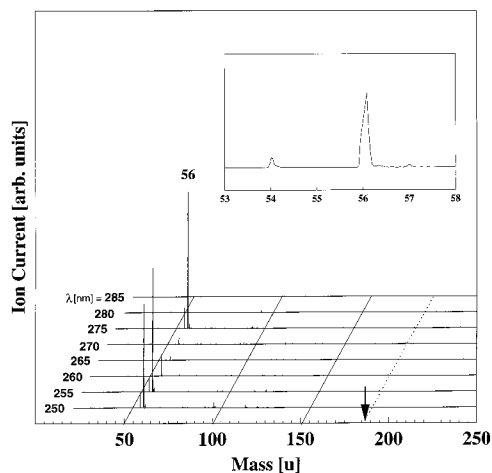


Figure 2. Multiphoton mass spectra of ferrocene recorded at different wavelengths. Note that no ferrocene cations at mass 186 u (marked by an arrow) were detected. The strong signal at 56 u is from Fe atoms produced by a fast dissociation of the neutral ferrocene after photoexcitation.

of the ferrocene derivatives and detecting the subsequent production of iron cations. Excitation and ionization of the ferrocene derivatives was achieved in a resonantly enhanced two-photon two-color process. The produced cations were accelerated in an electric potential of 1000 V toward the ion reflector, where they are reflected back toward the multi-channel plate ion detector. REMPI spectra are recorded mass selectively with a gated integrator/microcomputer system, and mass spectra were recorded by a LeCroy transient recorder system (TR8828).

3. Results

3.1. Ferrocene and [3]Ferrocenophane. Both ferrocene and [3]ferrocenophane (1,1'-trimethyleneferrocene) (see Figure 1, parts 1a and 1b) are building blocks of the investigated derivatives and act as electron donors in our experiment. The UV/VIS absorption spectra of both substances^{20–23} are nearly identical. In solution and in the gas phase both substances absorb light in a broad wavelength range below 400 nm, with some smooth features that have been assigned to d–d transitions in Fe, metal-to-ligand or ligand-to-metal charge transfer (MLCT or LMCT) transitions, and to electronic transitions within the cp rings.²⁰

To rule out the possibility of locally photoionizing the ferrocene or the [3]ferrocenophane molecule in a multiphoton process under the conditions of our experiment, we recorded laser mass spectra at different wavelengths, and resonant two-photon ionization (R2PI) spectra of the two compounds. Figure 2 displays a series of time-of-flight (TOF) mass spectra of ferrocene for several wavelengths of the excitation laser light. Clearly no intact parent molecule cations at the mass 186 u (ferrocene) but only Fe cations at the mass 56 u are found. The latter are produced in a subsequent multiphoton ionization process of Fe after decomposition of the photoexcited ferrocene. The inset of Figure 2 displays a magnified portion of the mass spectrum with a ⁵⁶Fe peak and the accompanying smaller isotopic ⁵⁴Fe peak.

For the [3]ferrocenophane we found the same results, i.e., strong Fe⁺ peaks but no signal at the parent mass (226 u). No mass spectrum is displayed, but in Figure 3 the recorded R2PI spectrum measured at mass 56 u (Fe⁺). The sharp lines are

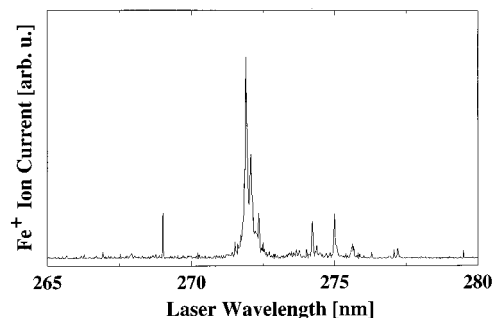


Figure 3. Resonance enhanced two-photon ionization spectrum of [3]ferrocenophane measured at the mass of Fe⁺ (56 u). The various lines indicate transitions in neutral Fe atoms produced by dissociation of photoexcited [3]ferrocenophane subsequently ionized by resonant two-photon ionization.

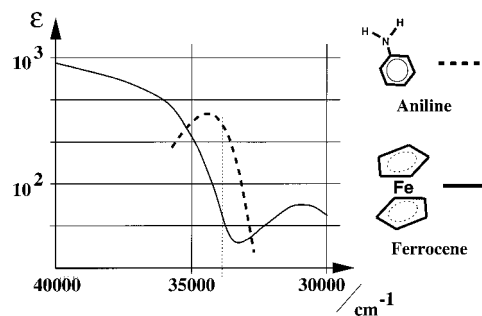


Figure 4. Schematic absorption spectra of ferrocene and aniline in solution. The absorption maximum of aniline is close to a minimum of absorption of ferrocene. The absorption coefficient ϵ is given in units of liter mol⁻¹ cm⁻¹. The dotted line denotes the S₁ ← S₀ transition of aniline at about 34 000 cm⁻¹.

transitions in the atomic Fe resulting from the resonance-enhanced two-photon ionization of the neutral Fe atoms produced after dissociation of the photoexcited ferrocenophane.

3.2. Derivatives. **3.2.1. *n*-(Ferrocenylmethyl)aniline.** In Figure 4 the absorption spectrum of aniline,²² which acts as a chromophore in the investigated derivatives, is schematically drawn and compared to a spectrum of ferrocene and ferrocenophane in the visible and near UV.²⁰ In the figure only the ferrocene spectrum is shown, because the spectra of ferrocene and ferrocenophane in solution and in the gas phase of these ferrocene compounds are very similar. At the left side to higher photon energies an absorption shoulder in the ferrocene spectrum can be identified, where the absorption coefficient increases by at least 1 order of magnitude within a relatively narrow frequency range of 2000 cm⁻¹. To lower energy a smaller maximum exists indicating the Fe d–d transition. The aniline S₁ ← S₀ transition maximum is located at about 34 000 cm⁻¹ at the right side of the absorption shoulder of pure ferrocene. At this frequency the absorption coefficient of ferrocene is substantially smaller than that of aniline.

A series of mass spectra of *n*-(ferrocenylmethyl)aniline is shown in Figure 5. They were recorded with the first (excitation) laser wavelength tuned to different values between 250 and 285 nm and the second (ionization) laser wavelength tuned to 350 nm. All mass peaks could be assigned unambiguously, as discussed below.

The most prominent feature in all traces is at mass 93 u. It is identified as aniline by its spectral fingerprint in a R2PI spectrum recorded at this mass. The aniline originates from minor thermal decomposition of the derivative in the heated nozzle. Because of the high sensitivity of laser mass spectrometry, the merest

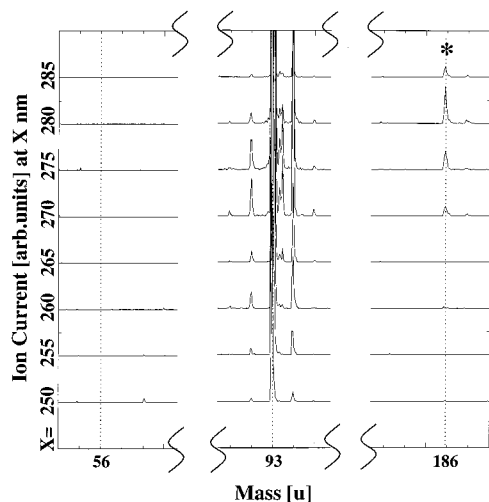


Figure 5. Multiphoton mass spectra of *n*-(ferrocenylmethyl)aniline (2a in Figure 1) recorded at different laser wavelengths. Note that no Fe cations at mass 56 u were detected. The strong aniline signal at mass 93 u is produced by thermal decomposition of the ferrocene derivative. The signal at mass 186 u marked with an asterisk originates from ferrocene cations produced by an intramolecular dissociative charge transfer. For explanation of the wavelength dependence, see text.

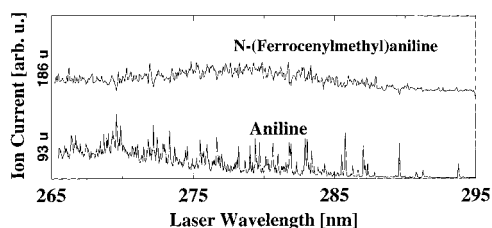


Figure 6. Resonance enhanced two-photon ionization spectra of *n*-(ferrocenylmethyl)aniline (2a in Figure 1), recorded at the mass of ferrocene (186 u, upper trace) and aniline (93 u, lower trace). Note the similarity of the position of the maximum in both spectra. For explanation, see text.

traces of aniline generate considerable signals. For the same reason, additional signals are observed originating from impurities and residuals of previous experiments in the nozzle.

We could not observe parent ions of the intact ferrocene derivative at the mass of 291 u, but, more important, a signal at the mass 186 u of ferrocene was found. There is no other reasonable combination of fragments and molecules which could explain the formation of a signal at this mass. So it is clear that this peak originates from ferrocene cations. The intensity of the ion current could be varied by tuning the laser intensity of the excitation or the ionization laser, so that this signal must originate from a true two-color process.

In addition to the mass spectra, resonant two-photon ionization (R2PI) spectra in the vicinity of the $S_1 \leftarrow S_0$ transition of aniline (294 nm) were recorded, varying the excitation wavelength while recording the signal at a mass of 93 u (aniline) and 186 u (ferrocene). The resulting two spectra in Figure 6 display some similarity in the position of the maximum. On the other hand the pure ferrocene absorption spectrum is completely different in the observed spectral range. The spectrum recorded at 186 u, i.e., the excitation spectrum of the ferrocene derivative, is substantially broadened and no distinct structure can be found. This is what we would expect when assuming that the energy levels of the chromophore aniline are disturbed and shifted by some intramolecular interactions with the ferrocene part of the molecule. Thus the intermediate state

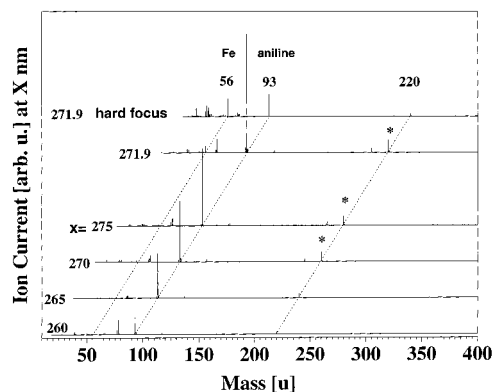


Figure 7. Multiphoton mass spectra of 2-(*n*-phenyl)amino-[3]-ferrocenophane (2b in Figure 1) recorded at different laser wavelengths. The signal at mass 93 u originates from aniline after thermal decomposition of the ferrocene derivative. Top trace: Fe cations at mass 56 u are present after fragmentation of the neutral ferrocene derivative by sharply focused laser light, tuned to atomic resonance of Fe at 271.9 nm. Lower traces: A mass peak at 220 u appears, marked with asterisks. For explanation, see text.

spectrum is a fingerprint of the absorption pathway via the aniline part of the ferrocene derivative.

3.2.2. 2-(*n*-Phenyl)amino-[3]-Ferrocenophane. Similar experiments as described above were performed with the bridged ferrocene-aniline derivative. As before, a series of mass spectra was recorded and the result is shown in Figure 7. Again, the strongest mass peaks originate from aniline. The total signal from this compound was weaker, since the 2-(*n*-phenyl)amino-[3]-ferrocenophane has a smaller vapor pressure than *n*-(ferrocenylmethyl)aniline. In contrast to the results obtained for *n*-(ferrocenylmethyl)aniline, here no signal at the mass 186 u (ferrocene) could be detected. Again, no parent ions of the intact derivative at the mass of 317 u could be observed. Instead, a signal at mass 220 u is detected. A large mass such as this can be only observed for a molecule or fragment containing a ferrocene subunit, since combinations of fragment or cluster masses do not yield a mass of 220 u.

4. Discussion

The main result of our experiments is that a signal at the ferrocene mass or at a mass larger than ferrocene is observed for the case of ferrocene-chromophore derivatives. This is completely different from the experiment with ferrocene molecules where absorption takes place in ferrocene itself leading to a strong dissociation and production of Fe^+ ions but no signal at all at the ferrocene mass. From this we conclude that the excitation and ionization mechanism is different for both experiments. In principle two excitation mechanisms are possible for our experimental conditions: (i) Ferrocene cations are produced by a charge transfer from aniline cations to ground state ferrocene molecules in a collision, similar to chemical ionization. Free aniline cations are produced by thermal decomposition of the derivatives in our experiment. It is likely that ferrocene molecules are produced in the same way. The aniline molecules are easily detected by REMPI and yield strong peaks at 93 u in the mass spectra of Figure 5. On the other hand ferrocene molecules present in the gas jet cannot be identified in the mass spectrum since they dissociate into Fe and cp rings in a MPD process before ionization. To check this process, special experiments with a mixture of ferrocene ($Fe(cp)_2$) and aniline in the molecular beam were carried out for the same laser conditions as used before. The mass spectra obtained after resonance-enhanced two-photon excitation at λ_1

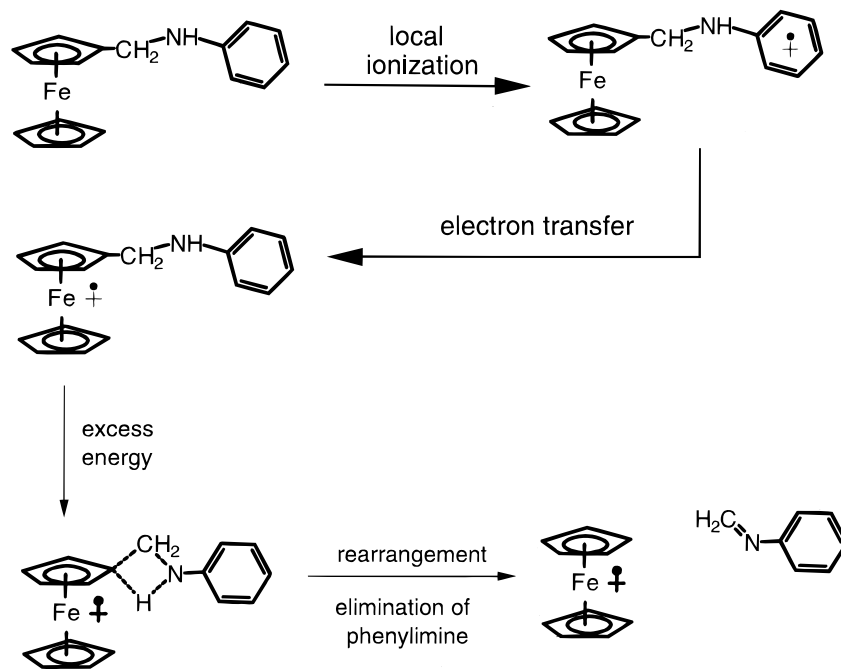


Figure 8. Excitation and dissociation pathway of *n*-(ferrocenylmethyl)aniline (2a in Figure 1). After local ionization of the aniline site electron transfer takes place from the ferrocene part to the aniline part followed by fragmentation of the compound. The excess energy released leads to a hydrogen transfer from the aniline to the ferrocene part, resulting in a formation of ferrocene⁺ as detected and a concomitant elimination of phenylimine.

in the range between 250 nm to 285 nm and $\lambda_2 = 350$ nm did not display any peak at the mass of ferrocene (186 u) and only iron (56 u) and aniline (93 u) cations were produced. From this result we conclude that an intermolecular charge transfer from aniline cations to ferrocene does not take place with sufficient efficiency and can be ruled out as a source for the appearance of ferrocene cations in the experiments with ferrocene-aniline derivatives described above. (ii) Therefore, we conclude that the ferrocene signal observed at 186 u originates from an intramolecular charge transfer following the excitation and ionization of the ferrocene derivative at the aniline site.

At this point we briefly discuss the site selective excitation in a ferrocene derivative containing a ferrocene and a chromophore site. If absorption of the first photon takes place at the absorption maximum of the aniline site with ns laser pulses the excitation of long-lived aniline zero order states is possible which are weakly coupled to the broad dissociative zero order states of the ferrocene site. For weak coupling the time evolution is so slow that the absorption of the second photon takes place from the aniline zero order state to the ionization continuum of the aniline. On the other hand an absorption from excited ferrocene zero order states is not possible since they rapidly decay by dissociation. The emitted electron is the π^* electron of the aniline leading to a local ionization of the aniline part of the molecule, i.e., an ionic wave function which is located at the aniline site and thus similar to the aniline⁺ MO function. The so produced ion zero order wave functions with aniline character are not eigenstates and develop in time to a final eigenstate of the system with positive charge localized at the ferrocene part of the molecule.²⁴ After this rapid charge transfer process, the difference of the local IEs of ferrocene and aniline, which is about 1 eV, is released.

As the charge transfer process is fast it occurs during the laser pulse duration (some ns). After the charge transfer additional photons can be absorbed, leading to a higher internal energy of the cation which is sufficient for forming finally the products shown in Figure 9, C and D, which are less stable than the initial structures A and B.

If the dissociation rate constant is fast, fragments are produced during the laser pulse which in turn can absorb further photons as was demonstrated first for the ladder switching process for benzene cations.^{25,26}

In Figures 8 and 9 possible pathways of the dissociative intramolecular charge-transfer reactions are shown. The primary step in the reaction of *n*-(ferrocenylmethyl)aniline (Figure 8) is the transfer of an electron from the ferrocene part to the ionized aniline part. Subsequently, the fragmentation of the compound proceeds. As a key step the excess energy released after the electron transfer leads to a hydrogen transfer from the aniline to the ferrocene part. Most likely the excess energy is sufficient for the hydrogen transfer and no energy take-up by absorption of further photons is necessary. This results in the formation of ionic ferrocene as detected and the concomitant elimination of phenylimine. Such a decomposition pathway is not found in the electron impact mass spectrum of the compound,²⁷ but it is reported as a minor route with other ferrocenylmethanamines and ferrocenylmethanol.^{27,28} The fragmentation pathway of complex 2b (see Figure 1) should not be as simple as in complex 2a (see Figure 1) because of its more complex structure. After ionization of the aniline, electron transfer is again assumed as the primary step to take place. This primary electron transfer step initiates a series of reactions. The aniline is eliminated by take-up of a hydrogen atom presumably from the alkyl bridge. The resulting ferrocene A (see Figure 9) could in principle rearrange to compound B which is known as a stable compound.¹⁷ A mass peak which corresponds to B is not found. The different fragmentation pathway leading to a cation of mass 220 u can be obtained by eliminating 4 hydrogen atoms from A and rearrangement to complex C. The formation of an alkyne residue and a fulvene ligand seems to be feasible since fulvene ligands are quite widespread in ferrocenylcarbenium chemistry.²⁹

It is also known from mass spectra of [3]-ferrocenophanes, that the interannular bridge is preferentially cleaved between the first and second carbon atom of the bridge and not between

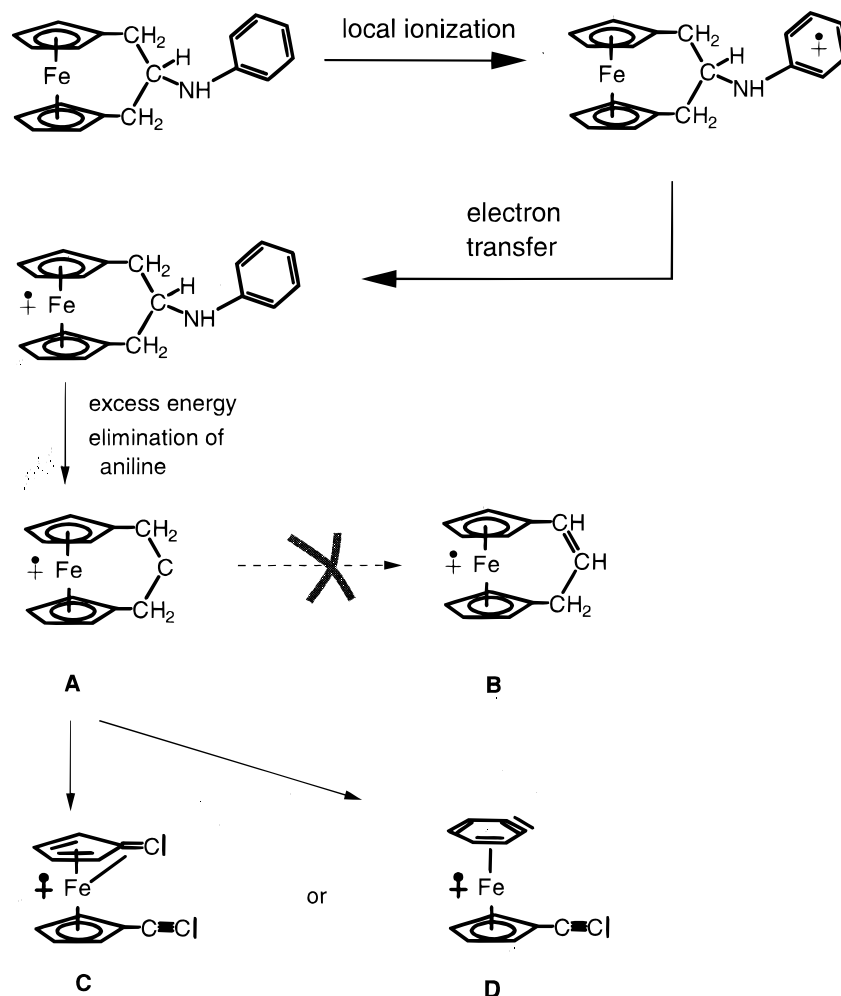


Figure 9. Excitation and dissociation pathway of 2-(*n*-phenyl)amino-[3]-ferrocenophane (2b in Figure 1). An electron transfer step initiates a series of reactions. Aniline is eliminated by take up of a hydrogen atom presumably from the alkyl bridge, resulting in ferrocene A. There are two possible fragmentation pathways. (i) Rearranging to compound B which is known as a stable compound,¹⁷ not found in our mass spectra. (ii) Elimination of 4 hydrogen atoms from A and rearrangement to complex C. Formation of an alkyne residue and a fulvene ligand seems to be feasible since fulvene ligands are quite widespread in ferrocenylcarbenium chemistry.²⁹ As an alternative one could think of the formation of an aryne ligand as described in structure D.

the cp-ligand and the first carbon atom.³⁰ As an alternative one could think of the formation of an aryne ligand as described in structure D.

Such ring expansions from cp to benzene derivatives are often found in mass spectra of ferrocenes.³⁰ From thermochemical estimates for structures C and D one can expect their formation to be only slightly endothermic, so that the absorption of one or more additional photons can deliver the energy needed for eliminating the hydrogen atoms.

The ferrocene peaks at 186 u in the mass spectra are not broadened. This would be the case for a dissociation time similar to the acceleration time in the ion optics. So we conclude that the dissociation occurs on a time scale much faster than 1 μ s, which is the typical time resolution of our mass spectrometer. In addition, from the energetic considerations above we conclude that the charge transfer process rate is faster than 10^8 s⁻¹ and thus occurs during the laser pulse.

5. Summary and Conclusion

Ferrocene molecules are typical examples for a fast dissociation in the excited electronic state. As a consequence in previous work no parent ions have been observed after resonance-enhanced two-photon ionization with UV light. In this work

novel ferrocene derivatives were investigated by resonance-enhanced time-of-flight laser mass spectrometry to study dissociative charge-transfer processes in isolated molecules, after optical excitation. The site-selective ionization of these molecules at the chromophore site results in a subsequent electron transfer from the ferrocene part to the chromophore part. The energy difference of about 1 eV between the local IEs and additional energy takeup by absorption of further laser photons lead to an excess energy sufficient for breaking the chemical bond between the two functional moieties. The appearance of ferrocene or ferrocene-containing cations is therefore explained by a fast ($<10^{-8}$ s) charge transfer process between the two parts of the ferrocene derivatives after local ionization and a subsequent dissociation.

Future experiments will include the dependence of the charge transfer rate on the distance of the moieties and the difference of the ionization energies. This information is expected by varying the distance between the ferrocene and the chromophore or by the use of specially synthesized ferrocene-chromophore derivatives with varying IEs and absorption spectra.

Acknowledgment. This work was supported by the SFB 377, "Photoionisation und Ladungstrennung in großen Molekülen, Clustern und kondensierter Phase" and the Fonds der

Chemischen Industrie. The authors would like to thank Dr. Klaus Latzel and Felix Bauer for experimental support and helpful discussions.

References and Notes

- (1) Togni, A.; Hayashi, T. *Ferrocenes*, 1st ed.; VCH: Weinheim, New York, 1995.
- (2) Kealey, T. J.; Pauson, P. L. *Nature* **1951**, *168*, 1039.
- (3) Astruc, D. *Electron Transfer and Radical Processes in Transition-Metal Chemistry*, 1st ed.; VCH: Weinheim, New York, 1995.
- (4) Leutwyler, S.; Even, U.; Jortner, J. *Chem. Phys. Lett.* **1980**, *74*, 11.
- (5) Engelking, P. C. *Chem. Phys. Lett.* **1980**, *74*, 207.
- (6) Leutwyler, S.; Even, U.; Jortner, J. *J. Phys. Chem.* **1981**, *85*, 3026.
- (7) Bär, R.; Heinis, Th.; Nager, Ch.; Jungen, M. *Chem. Phys. Lett.* **1982**, *91*, 440.
- (8) Nagano, Y.; Achiba, Y.; Kimura, K. *J. Phys. Chem.* **1986**, *90*, 1288.
- (9) Liou, H. T.; Ono, Y.; Engelking, P. C.; Moseley, J. T. *J. Phys. Chem.* **1986**, *90*, 2888.
- (10) Liou, H. T.; Engelking, P. C.; Ono, Y.; Moseley, J. T. *J. Phys. Chem.* **1986**, *90*, 2892.
- (11) Ray, U.; Hui, H. Q.; Zhang, Z.; Schwarz, W.; Vernon, M. *J. Chem. Phys.* **1989**, *90*, 4248.
- (12) Opitz, J.; Härter, P. *Int. J. Mass. Spectrom. Ion. Proc.* **1992**, *121*, 183.
- (13) Connor, J. A. *Top. Curr. Chem.* **1977**, *71*, 71.
- (14) Wilkinson, G.; Pauson, P. L.; Cotton, F. A. *J. Am. Chem. Soc.* **1954**, *76*, 1970.
- (15) Rabalais, J. W.; Werme, L. O.; Bergmark, T.; Karlsson, L.; Hussain, M.; Siegbahn, K. *J. Chem. Phys.* **1972**, *57*, 1185.
- (16) Pennie, J. T.; Bieber, T. I. *Tetrahedron Lett.* **1972**, *34*, 3535.
- (17) Sonoda, A.; Moritani, I. *J. Organomet. Chem.* **1971**, *26*, 133.
- (18) Grebner, Th. L.; Neusser, H. J. *Chem. Phys. Lett.* **1995**, *245*, 578.
- (19) Ernstberger, B.; Krause, H.; Kiermeier, A.; Neusser, H. J. *J. Chem. Phys.* **1990**, *92*, 5285.
- (20) Armstrong, A. T.; Smith, F.; Elder, E.; McGlynn, S. P. *J. Chem. Phys.* **1967**, *46*, 4321.
- (21) Sohn, Y. S.; Hendrickson, D. N.; Gray, H. B. *J. Am. Chem. Soc.* **1971**, *93*, 3603.
- (22) Perkampus H.-H. *UV-Vis Atlas of Organic Compounds Part II*, 2nd ed.; VCH: New York, 1992.
- (23) Rosenblum, M.; Banerjee, A. K.; Danieli, N.; Fish, R. W.; Schlatter, V. *J. Am. Chem. Soc.* **1963**, *85*, 316.
- (24) Cederbaum, L. S.; Zobeley, J. *Chem. Phys. Lett.* **1999**, *307*, 205.
- (25) Boesl, U.; Neusser, H. J.; Schlag, E. W. *J. Chem. Phys.* **1980**, *72*, 4327.
- (26) Dietz, W.; Neusser, H. J.; Boesl, U.; Schlag, E. W.; Lin, S. H. *Chem. Phys.* **1982**, *66*, 105.
- (27) Beckwith, A. L. J.; Vickery, G. G. *J. Chem. Soc., Perkin Trans. I* **1975**, *18*, 1818.
- (28) Budzikiewicz, H.; Djerassi, C.; Williams, D. H. *Mass Spectrometry of Organic Compounds*; Holden-Day: New York, 1967.
- (29) Elschenbroich, Ch.; Salzer, A. *Organometalchemie*; Teubner, 1988.
- (30) Cais, M.; Lupin, M. S. *Adv. Organomet. Chem.* **1970**, *8*, 211.